

Optic axial angle, a precise measure of Al,Si ordering in T₁ tetrahedral sites of K-rich alkali feldspars

S. C. Su,¹ F. D. BLOSS, P. H. RIBBE

Department of Geological Sciences
Virginia Polytechnic Institute and State University
Blacksburg, Virginia 24061

AND D. B. STEWART

U. S. Geological Survey
959 National Center, Reston, Virginia 22092

Abstract

For most K-rich alkali feldspars, the optic axial angle $2V_x$ provides a precise estimate of the total Al content ($= \Sigma t_1$) of the T₁ tetrahedral sites. For monoclinic varieties with the optic axial plane (OAP) parallel to (010),

$$\Sigma t_1 = 2t_1 = 0.665 - 0.711 \sin^2 V_x.$$

For monoclinic varieties with the OAP perpendicular to (010) and for triclinic varieties with the OAP nearly perpendicular to (010),

$$\Sigma t_1 = t_{1o} + t_{1m} = 0.665 + 0.711 \sin^2 V_x.$$

These equations represent two segments of a line derived by least-squares regression performed on literature data for 52 specimens (19 with structural refinements) for which Σt_1 values were calculated from cell parameters using the [110],[1 $\bar{1}$ 0] method of Kroll (1980). The standard error of estimate is 0.02; $r^2 = 0.962$. Thus by use of a spindle stage or universal stage, one can rapidly and precisely determine the "structural state" for individual grains or, in thin sections, from point to point in a single grain. For the feldspars used in the regression, no account was taken of their symmetry, of the albite content (up to 20 mol %), of minor amounts of Ca, Ba, Sr, or Fe, or of the possible effects of strain or submicroscopic twinning or exsolution, indicating that these factors may be disregarded in using these equations.

The changes in optic orientation and $2V_x$ as Al,Si order increases from high sanidine [OAP = (010)] to orthoclase [OAP \perp (010)] to low microcline [OAP $\sim \perp$ (010)] are explained by assuming a simple *linear* variation in principal refractive indices with structural state.

Introduction

It is well known that the optic axial angle $2V_x$ is strongly dependent on the long-range order of Al,Si in the tetrahedral sites of K-rich feldspars, and in fact $2V_x$ has been used to designate relative "structural states" for many years (see Smith, 1974, Chapter 8, for a review). Conventionally, the highly disordered, monoclinic *high sanidines* (HS) have optic axial planes (OAP's) parallel to (010) with $2V_x$ ranging from $\sim 60^\circ$ to 0° ; *low sanidines* (LS) have OAP's normal to (010) with $0^\circ < 2V_x < \sim 36^\circ$;

orthoclases (OR) also have OAP's \perp (010), but with $\sim 36^\circ < 2V_x < \sim 80^\circ$. Triclinic *microclines* (MC) have OAP's approximately normal to (010) with $2V_x$ values overlapping the orthoclases and vary from $\sim 38^\circ$ (*intermediate microclines*) to $\sim 85^\circ$ for completely ordered *low* or *maximum microcline* (LM).² Thus, combined with the change in orientation of the optic plane, $2V_x$ varies through a

¹ Permanent address: Institute of Geology, Chinese Academy of Sciences, Beijing, The People's Republic of China.

² Optically positive microclines ("iso-microclines") have been reported, but we have examined the specimens of Blasi (1972) by microprobe X-ray scanning methods and found them to be mechanical mixtures of exsolved low microcline ($2V_x \approx 85^\circ$) and low albite ($2V_x \approx 103^\circ$). For a detailed review of alkali feldspar optics, see Stewart and Ribbe (1983).

total of 145° as Al,Si ranges from disordered to ordered in K-rich alkali feldspars.

The crystal structures of potassic feldspars are well documented by 15 or more modern structural refinements of $C2/m$ sanidines and orthoclases and another 15 of $C\bar{1}$ microclines. These have led to a detailed understanding of the response of unit cell parameters—notably b , c , α^* and γ^* —to changes in Al,Si distribution within the two tetrahedral sites (T_1 and T_2) of monoclinic potassic feldspars and among the four tetrahedral sites (T_{1o} , T_{1m} , T_{2o} and T_{2m}) of triclinic ones. Using the symbols t_1 , t_2 , t_{1o} , t_{1m} , t_{2o} and t_{2m} to designate the average Al/(Al + Si) contents of these sites (as determined from mean T–O bond lengths in the aforementioned structural refinements), we may make the following statements about K-rich alkali feldspars: (1) For $C2/m$ monoclinic specimens: $2t_1 + 2t_2 = 1.0$. (2) For $C\bar{1}$ triclinic specimens: $t_{1o} + t_{1m} + t_{2o} + t_{2m} = 1.0$. (3) The most disordered high sanidine has $2t_1 = 2t_2 = 0.5$ (although this has never been observed in a natural specimen). (4) In low sanidines and orthoclases $2t_1$ becomes increasingly greater than $2t_2$ as ordering increases. (5) Microclines have $t_{1o} > t_{1m} > t_{2o} = t_{2m}$ or $t_{1o} > t_{1m} = t_{2o} = t_{2m}$. (6) Ordered low microcline has $t_{1o} = 1.0$, $t_{1m} = t_{2o} = t_{2m} = 0.0$. Kroll and Ribbe (1983) give details on how to estimate Al contents of T sites from crystal structure data and from unit cell parameters determined by X-ray single-crystal or powder diffractometry. In this paper, however, we present the *quantitative* relationship between the total Al content of the T_1 sites, $\Sigma t_1 = 2t_1$ or $(t_{1o} + t_{1m})$, and $2V_x$, thus establishing a rapid and precise method of determining the structural state of separated grains of K-rich alkali feldspars (using a spindle stage) or from point to point on grains in thin section (using a universal stage).

The relation of optical properties to Al,Si distribution

Disordered high sanidine ($\Sigma t_1 \approx 0.5$) and ordered low microcline ($\Sigma t_1 \approx 1.0$) differ markedly in optic orientation (Fig. 1). Consequently, to facilitate comparison of principal refractive indices for light vibrating along *similar* crystallographic directions in these two structures (and in those of intermediate structural states), we use n_b to symbolize the principal index for light vibrating parallel or nearly parallel to the crystallographic axis b . In this we follow Hewlett (1959), who used the symbol "b" (see also Finney and Bailey, 1964). We extend this convention by using n_a and n_c to indicate the principal refractive indices for light vibrating most nearly parallel to the a and c crystallographic axes, respectively, even though these vibrations may be at appreciable angles to a and c .

Refractive indices versus unit cell edges

If at opposite ends of a "structural state" scale we plot the principal refractive indices for high sanidine (HS) and low microcline (LM) and label them n_a , n_b , n_c instead of

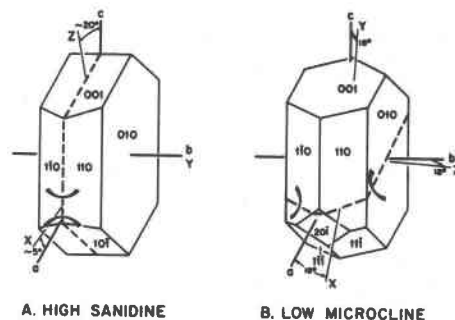


Fig. 1. The optic orientations of high sanidine and low microcline. Dashed lines are the traces of the optic axial planes.

α , β , γ , and if we simplistically assume that n_a , n_b and n_c vary linearly with total Al content of the T_1 sites, the lower portion of Figure 2 results. The general correctness of this model over that in which γ_{HS} is traditionally connected to γ_{LM} and β_{HS} to β_{LM} , is readily apparent. It indicates that, for OAP = (010) in HS, $2V_x$ decreases from $\sim 60^\circ$ to 0° with increased Al,Si ordering. With continued Al,Si ordering beyond the point where n_b equals n_c , the OAP becomes perpendicular to (010) or nearly so, and $2V_x$ increases from 0° toward its maximum value of $\sim 85^\circ$ for LM. Cell-edge data for HS and LM also corroborate this model. If we add these data to Figure 2 and for simplicity assume linear variation, we note a reciprocal relationship between each cell edge and the principal refractive index for light vibrating most nearly parallel to it. Thus, as Al,Si ordering increases from HS to LM, a marked increase in n_b accompanies a marked decrease in b , a slight increase in n_a accompanies a slight decrease in a , and a marked decrease in n_c accompanies a marked increase in c . This principle of the inverse relationship between cell-edge length and corresponding refractive index was first demonstrated convincingly for the andalusite–kanonaite series by Gunter and Bloss (1982) and, indeed, aided our insight into the alkali feldspars. In Figure 2 we arbitrarily chose to plot b and c so that they cross at the Σt_1 value for which $n_b = n_c$ in our model. This emphasizes the reciprocity between the refractive index and its corresponding cell edge by causing the triangles formed by the intersection of lines b and c to be very similar to the two formed by the intersection of lines n_c and n_b .

Hewlett (1959) recognized that the d_{010} and d_{001} spacings varied nearly linearly with structural state of K-rich feldspars, and Stewart and Ribbe (1969) quantified these relationships for the b and c cell edges of all alkali feldspars. In Figure 3 it can be seen that the Al contents encountered in any six contiguous tetrahedral sites along b ($\equiv Al_b$) and any three along c ($\equiv Al_c$) are:

$$Al_b = t_{1o} + t_{1m} + 4t_2, \quad (1)$$

and

$$Al_c = t_{1o} + t_{1m} + t_2, \quad (2)$$

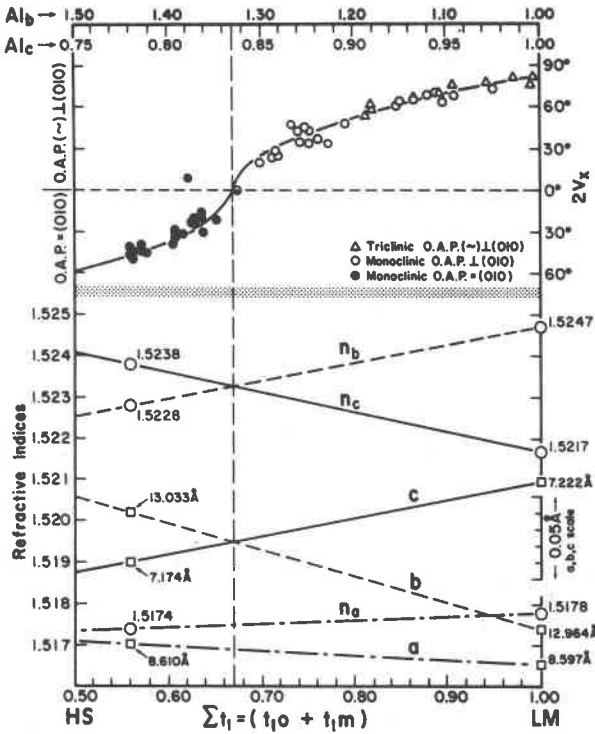


Fig. 2. The refractive indices, n_a , n_b , n_c (open circles), and unit cell dimensions, a , b , c , (open squares), are plotted for high sanidine (HS) and low microcline (LM), and simple linear variations are assumed for each parameter. The n values for HS were determined by refinement of values extrapolated from data given by Smith (1974, Figs. 8–9, p. 386); the corresponding $2V_x = 46.4^\circ$. The n values for LM are those of the Pellotsalo specimen of Brown and Bailey (1964); $2V_x = 82.3^\circ$. The cell dimensions of HS ($t_{10} = 0.56$) and LM ($t_{10} = 1.0$) are those chosen by Kroll and Ribbe (1983) as standard reference values for alkali feldspars [see their paper (pp. 71 and 74 and Table 4) for details and reasons for choosing to plot HS at $\Sigma t_1 = 0.56$; this choice controls the values of α_s , β_s , γ_s , and the coefficients in Equations 8 and 9]. The Al_b , Al_c (upper abscissa) and Σt_1 (lower abscissa) scales are linearly related (Equations 4 and 5). The sigmoidal curve of $2V_x$ versus Σt_1 was calculated in the manner described in the text; data from Table 1 were subsequently added. For an earlier version, see Su *et al.* (1983a).

where t_2 represents t_{20} or t_{2m} for triclinic feldspars (in which all structure analyses to date have shown $t_{20} = t_{2m}$). Because

$$t_{10} + t_{1m} + t_{20} + t_{2m} = 1$$

$$\text{or } \Sigma t_1 + t_{20} + t_{2m} = 1,$$

and since $t_{20} = t_{2m}$,

$$t_2 = \frac{1}{2}(1 - \Sigma t_1). \tag{3}$$

Equations 1 and 2 may be rewritten

$$Al_b = \Sigma t_1 + 2(1 - \Sigma t_1) = 2 - \Sigma t_1, \tag{4}$$

and

$$Al_c = \Sigma t_1 + (1 - \Sigma t_1)/2 = (1 + \Sigma t_1)/2. \tag{5}$$

To a first approximation, therefore, the amounts of Al encountered along b and c are linear functions of Σt_1 (see upper abscissa in Fig. 2), Al_b decreasing from 1.5 for HS to 1.0 for LM and Al_c increasing exactly half as much, that is, from 0.75 for HS to 1.0 for LM. Because the effective size of Al is larger than Si (mean T–O bonds are $\sim 1.74\text{\AA}$ for Al sites, $\sim 1.61\text{\AA}$ for Si sites), Stewart and Ribbe (1969) were able to show that the cell edges b and c vary proportionately with Σt_1 , as now confirmed by approximately 30 crystal structures (Kroll and Ribbe, 1983). By contrast, the cell edge a varies only slightly with Al,Si ordering because

$$Al_a = t_{10} + t_{1m} + t_{20} + t_{2m} = 1.0,$$

and the actual distribution of Al among these sites is essentially irrelevant to the length of a .

Sigmoidal $2V_x$ curve

We now assume that the refractive indices and their linear variation with Al,Si ordering are reasonably correct (Fig. 2). From these refractive index trends, we can

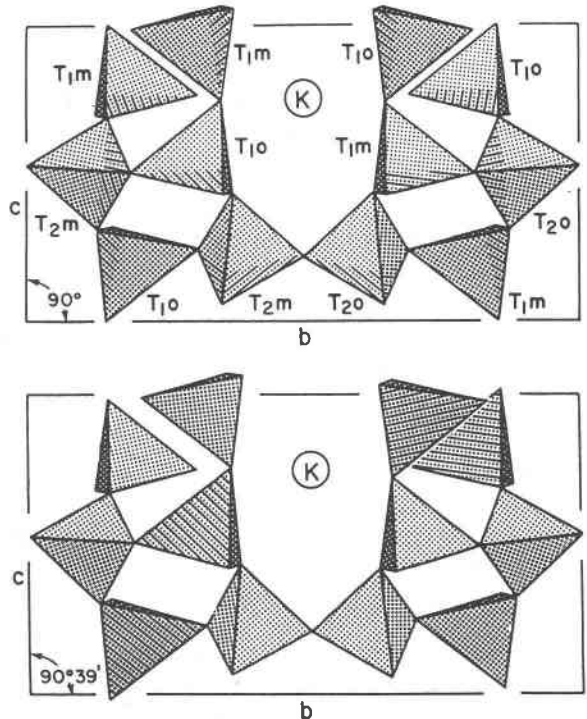


Fig. 3. The arrangement of tetrahedra along b and c in similar regions of the unit cells of high sanidine (HS) and low microcline (LM). The tetrahedra are ruled roughly in proportion to their Al content (0.25 for each T site in HS; 1.0 for T_{10} in ordered LM).

calculate $2V_x$ using the exact equation

$$\sin^2 V_x = \frac{\beta^{-2} - \gamma^{-2}}{\alpha^{-2} - \gamma^{-2}} \quad (6)$$

or, to within a few tenths of a degree for crystals of low birefringence like potassic feldspars, using the approximate equation

$$\sin^2 V_x \approx \frac{\gamma - \beta}{\gamma - \alpha} \quad (7)$$

Plotting $2V_x$ values calculated from the linearly varying refractive indices against Σt_1 produces the sigmoidal curve shown near the top of Figure 2. To this curve we

$$\Sigma t_1 = 0.44 \left[\frac{(\gamma_s - \beta_s) - (\gamma_s - \alpha_s) \sin^2 V_x}{[(\gamma_m - \beta_m) + (\gamma_s - \beta_s)] + [(\beta_m - \alpha_m) - (\gamma_s - \alpha_s)] \sin^2 V_x} \right] + 0.56 \quad (8)$$

For $\text{OAP} \perp (010)$ or $\sim \perp (010)$ we obtain:

$$\Sigma t_1 = 0.44 \left[\frac{(\gamma_s - \beta_s) - (\beta_s + \alpha_s) \sin^2 V_x}{[(\gamma_m - \beta_m) + (\gamma_s - \beta_s)] + [(\gamma_m - \alpha_m) - (\beta_s - \alpha_s)] \sin^2 V_x} \right] + 0.56 \quad (9)$$

added data from the literature for which $2V_x$ and unit cell parameters were both reported (Table 1) so that t_{10} and t_{1m} could be calculated for each specimen using the $[110], [1\bar{1}0]$ translation method of Kroll (1980, reported in Kroll and Ribbe, 1983). Most of these data points fall very close to the sigmoidal curve. In fact, the estimated standard error in Σt_1 is 0.02 for 52 specimens, 19 of which have known crystal structures that confirm the Σt_1 values calculated by Kroll's method (see Table 2).

The agreement between the sigmoidal model and the crystal data is all the more remarkable because: (1) No consideration was given to whether the crystal symmetry was monoclinic or triclinic; (2) No correction for albite content was made even though some specimens contained up to 20 mol % Ab, in addition to minor amounts of Ca, Ba, Sr, and Fe; (3) Some of the specimens are submicroscopically twinned and/or exsolved; (4) Some specimens may be strained; (5) The sigmoidal curve, in the final analysis, was derived from just two sets of data points (HS and LM; data on Fig. 2) together with the simplistic assumption that refractive indices n_a , n_b and n_c vary linearly with Al,Si ordering between HS and LM; (6) For 32 of these data, cell parameters were measured on powdered specimens and $2V_x$ on separate crystals, and even some of the specimens whose crystal structures were determined had their $2V_x$ values measured on separate single crystals. Only eight of the nine feldspars in the superb suite of Dal Negro et al. (1978) and DePieri (1979) are certain to have had $2V_x$ and Σt_1 (from both cell parameters and structure analyses) measured on the same grain! In fact, some of the specimens in Table 1 had $2V_x$ measured by Spencer (1937) and cell parameters mea-

sured by powder methods on the K-rich phase only (Stewart and Wright, 1974); these parameters were used to calculate Σt_1 . Since "geologic evidence is abundant for a range in $2V_x$ of tens of degrees in one feldspar crystal, and of 50° or more among the crystals in a single hand specimen" (Stewart and Ribbe, 1983, p. 133), it is remarkable how good the agreement is with the sigmoidal curve.

A corollary of the assumed linear variation of n_a , n_b and n_c relative to Σt_1 (Fig. 2) is that the birefringences $(\gamma - \alpha)$, $(\gamma - \beta)$ and $(\beta - \alpha)$ also vary linearly with Σt_1 . These linear relationships, if used in conjunction with equation 6, will lead to the following general equations for the sigmoidal curve (after considerable mathematical manipulation). Thus, for $\text{OAP} = (010)$ we obtain:

Here the subscripts s and m respectively are abbreviations for HS and LM. To the extent that the refractive index data plotted in Figure 2 are correct, equation 8 becomes

$$\Sigma t_1 = 1.686 - \frac{1.626}{1.600 - \sin^2 V_x}, \quad (10)$$

and equation 9 becomes

$$\Sigma t_1 = -1.024 + \frac{4.517}{2.667 - \sin^2 V_x}. \quad (11)$$

Also, to the extent these refractive indices and equations 10 and 11 are valid, the cross-over point of the sigmoidal curve (i.e., the point where $V_x = 0^\circ$) occurs at $\Sigma t_1 = 0.67$.

Linear model: Σt_1 versus $\sin^2 V_x$

Equation 7 indicates that $\sin^2 V_x$ represents the quotient of two birefringences. Even if both birefringences vary linearly with Σt_1 , their quotient and thus $\sin^2 V_x$ would not do so (see the discussion by Bloss, 1952). Equations 10 and 11 also indicate that Σt_1 is related nonlinearly to $\sin^2 V_x$. Nevertheless, given the magnitude of the coefficients in Equations 10 and 11, and the fact that $0^\circ \leq V_x \leq 45^\circ$ so that $0 \leq \sin^2 V_x \leq 0.5$, the relationship between Σt_1 and $\sin^2 V_x$ is nearly linear. This explains why a linear regression performed on the data on Table 1, using $\sin^2 V_x$ as the independent variable and Σt_1 as the dependent variable, yields a coefficient of determination, $r^2 = 0.962$

Table 1. Potassium-rich alkali feldspars, their compositions (in mol % Or), $2V_x$ values and unit cell dimensions. For $2V_x$, a minus sign indicates that the optic axial plane is parallel to (010). Var = structural classification: MC = microcline, OR = orthoclase, LS = low sanidine, HS = high sanidine. As asterisk indicates the feldspar is metrically monoclinic, but topochemically triclinic. Ref = references, as listed at the bottom of the table.

#	Specimen	Mole % Or	Var	$2V_x$	a , Å	b , Å	c , Å	α (°)	β (°)	γ (°)	Ref
1	PELLOTSALO	95.0	MC	82.5	8.560	12.964	7.215	90.65	115.83	87.70	2
2	CA1E	88.6	MC	82.0	8.558	12.963	7.217	90.52	115.93	87.98	4
3	RC20C	85.5	MC	78.5	8.566	12.961	7.217	90.43	116.00	88.48	4
4	PONTISKALK	98.0	MC	77.0	8.573	12.962	7.218	90.57	115.92	87.75	5
5	SP-U	87.6	MC	76.0	8.578	12.960	7.211	90.30	115.97	89.12	1
6	P1C	90.0	MC	71.0	8.574	12.971	7.212	90.33	116.03	88.78	4
7	CA1B	88.6	MC	65.0	8.559	12.976	7.211	90.30	116.03	89.02	4
8	SP-H	86.3	MC	61.5	8.577	12.963	7.190	90.26	116.06	89.48	9
9	A1D	90.4	MC	53.0	8.563	12.984	7.201	90.13	116.02	89.50	4
10	SP-M	85.6	OR	73.7	8.637	12.895	7.185	90.00	116.24	90.00	9
11	SP-Z	90.1	OR	71.8	8.570	12.965	7.207	90.00	116.03	90.00	9
12	SP-I	90.2	OR	69.1	8.622	12.927	7.192	90.00	116.15	90.00	9
13	SP-B	90.0	OR	68.5	8.554	12.970	7.207	90.00	116.01	90.00	11
14	7007	88.1	OR	65.0	8.545	12.967	7.201	90.00	116.00	90.00	6
15	SP-V	90.7	OR	63.5	8.571	12.973	7.202	90.00	116.01	90.00	9
16	HIMALAYA	88.1	OR	63.0	8.563	12.963	7.210	90.00	116.07	90.00	8
17	SP-K	88.3	OR	61.4	8.605	12.944	7.186	90.00	116.10	90.00	9
18	CA1A	88.6	OR*	60.0	8.563	12.984	7.204	90.00	116.03	90.00	4
19	P2A	93.1	OR*	49.0	8.583	12.989	7.202	90.00	116.05	90.00	4
20	SP-F	74.9	OR	49.0	8.522	12.976	7.183	90.00	116.11	90.00	9
21	SP-D	80.5	OR	46.2	8.538	12.982	7.185	90.00	116.02	90.00	9
22	P50-56	87.7	OR	44.0	8.561	12.995	7.194	90.00	115.99	90.00	11
23	SP-C	90.8	OR*	43.6	8.562	12.996	7.193	90.00	116.01	90.00	3
24	P2B	93.1	OR	38.0	8.589	12.995	7.198	90.00	116.02	90.00	4
25	SP-A	93.9	OR	34.8	8.582	12.989	7.198	90.00	116.04	90.00	9
26	2B11-1	95.0	LS	35.0	8.574	13.003	7.199	90.00	116.02	90.00	7
27	2B31	92.0	LS	34.0	8.567	12.997	7.199	90.00	116.05	90.00	7
28	2B131	92.0	LS	28.0	8.568	13.004	7.195	90.00	116.04	90.00	7
29	2B12	94.0	LS	26.0	8.573	13.005	7.195	90.00	116.02	90.00	7
30	2B11-2	92.0	LS	25.0	8.569	13.003	7.192	90.00	116.02	90.00	7
31	2B6	94.0	LS	20.0	8.573	13.008	7.194	90.00	116.04	90.00	7
32	SV-17	90.0	LS	9.0	8.549	13.028	7.188	90.00	116.02	90.00	10
33	2B15-1	93.0	HS	0.0	8.572	13.011	7.190	90.00	116.03	90.00	7
34	S1A43-1	90.0	HS	-15.0	8.555	13.020	7.185	90.00	115.99	90.00	12
35	2B15-2	95.0	HS	-16.0	8.574	13.014	7.191	90.00	116.01	90.00	7
36	S1A33-1	91.0	HS	-20.0	8.557	13.024	7.184	90.00	115.97	90.00	12
37	2B4-1	93.0	HS	-20.0	8.574	13.017	7.185	90.00	116.03	90.00	7
38	2B4-2	93.0	HS	-22.0	8.570	13.018	7.188	90.00	116.01	90.00	7
39	7002	85.4	HS	-22.0	8.539	13.015	7.179	90.00	115.99	90.00	6
40	S1A44-1	89.0	HS	-24.0	8.553	13.021	7.183	90.00	115.98	90.00	12
41	S1A43-2	90.0	HS	-28.0	8.554	13.025	7.181	90.00	115.98	90.00	12
42	S1A33-2	91.0	HS	-30.0	8.558	13.025	7.182	90.00	115.99	90.00	12
43	2A4	93.0	HS	-30.0	8.570	13.017	7.186	90.00	116.04	90.00	7
44	S1A43-3	88.0	HS	-31.0	8.554	13.019	7.180	90.00	116.00	90.00	12
45	S1A44-2	89.0	HS	-34.0	8.555	13.023	7.181	90.00	116.00	90.00	12
46	S1A43-4	90.0	HS	-38.0	8.555	13.026	7.180	90.00	115.96	90.00	12
47	S1A33-3	89.0	HS	-39.0	8.551	13.032	7.179	90.00	116.00	90.00	12
48	SV-17T	89.0	HS	-41.0	8.546	13.037	7.178	90.00	115.97	90.00	10
49	S1A33-4	90.0	HS	-44.0	8.558	13.032	7.177	90.00	115.97	90.00	12
50	SAN-SP-C	90.8	HS	-44.5	8.565	13.030	7.175	90.00	115.99	90.00	3
51	1B1	92.0	HS	-45.0	8.567	13.031	7.181	90.00	116.03	90.00	7
52	5A1	94.0	HS	-50.0	8.574	13.032	7.178	90.00	116.02	90.00	7

1 Bailey (1969)	5 Finney & Bailey (1964)	9 Stewart (1974)
2 Brown & Bailey (1964)	6 Phillips & Ribbe (1973)	10 Weitz (1972)
3 Cole et al. (1949)	7 Priess (1982)	11 Wright & Stewart (1968)
4 DePieri (1979)	8 Prince et al. (1973)	12 Zeipert & Wondratschek (1981)

(see Fig. 4). The resulting equation is split into two segments. For OAP = (010),

$$\Sigma t_1 = 0.665(3) - 0.711(17) \sin^2 V_x, \quad (12a)$$

and for OAP perpendicular to (010), or nearly so

$$\Sigma t_1 = 0.665(3) + 0.711(17) \sin^2 V_x, \quad (12b)$$

with numbers in parentheses referring to the estimated

Table 2. The Al/(Al + Si) contents of the t_1 sites of specimens in Table 1. Column 1 = Σt_1 as determined from mean T-O bond lengths using structural data (Kroll and Ribbe, 1983, Tables 2 and 3). Column 2 = Σt_1 calculated by the [110],[110] method of Kroll (1980). Column 3 = Σt_1 predicted by our sigmoidal model. Column 4 is the residual of [column 2 - column 3], subject to round-off errors. Column 5 = Σt_1 predicted by our linear model. Column 6 = [column 2 - column 5].

#	Specimen	$2V_x$	1	2	3	4	5	6
1	PELLOTSALO	82.5	1.015	1.00	1.00	-0.00	0.97	0.02
2	CA1E	82.0	0.965	0.97	1.00	-0.02	0.97	0.00
3	RC20C	78.5	0.960	0.94	0.97	-0.02	0.95	-0.01
4	PONTISKALK	77.0	0.985	0.99	0.96	0.03	0.94	0.05
5	SP-U	76.0	0.910	0.91	0.95	-0.04	0.93	-0.03
6	P1C	71.0	0.870	0.90	0.92	-0.02	0.90	-0.01
7	CA1B	65.0	0.900	0.87	0.88	-0.00	0.87	0.00
8	SP-H	61.5	.	0.82	0.85	-0.04	0.85	-0.03
9	A1D	53.0	0.820	0.81	0.81	0.01	0.81	0.01
10	SP-M	73.7	.	0.95	0.93	0.02	0.92	0.03
11	SP-Z	71.8	.	0.89	0.92	-0.03	0.91	-0.02
12	SP-I	69.1	.	0.91	0.90	0.01	0.89	0.02
13	SP-B	68.5	0.830	0.88	0.90	-0.02	0.89	-0.01
14	7007	65.0	0.850	0.87	0.88	-0.01	0.87	-0.00
15	SP-V	63.5	.	0.85	0.87	-0.02	0.86	-0.01
16	HIMALAYA	63.0	0.900	0.90	0.86	0.03	0.86	0.04
17	SP-K	61.4	.	0.85	0.85	-0.01	0.85	-0.01
18	CA1A	60.0	0.840	0.82	0.85	-0.03	0.84	-0.02
19	P2A	49.0	0.775	0.79	0.79	0.00	0.79	0.00
20	SP-F	49.0	.	0.73	0.79	-0.05	0.79	-0.05
21	SP-D	46.2	.	0.75	0.77	-0.03	0.77	-0.03
22	P50-56	44.0	.	0.75	0.76	-0.01	0.76	-0.01
23	SP-C	43.6	0.720	0.74	0.76	-0.02	0.76	-0.02
24	P2B	38.0	0.725	0.76	0.74	0.02	0.74	0.02
25	SP-A	34.8	.	0.77	0.73	0.05	0.73	0.05
26	2B11-1	35.0	.	0.74	0.73	0.01	0.73	0.01
27	2B31	34.0	.	0.75	0.73	0.03	0.73	0.03
28	2B131	28.0	.	0.72	0.71	0.01	0.71	0.01
29	2B12	26.0	.	0.72	0.70	0.02	0.70	0.02
30	2B11-2	25.0	.	0.71	0.70	0.01	0.70	0.01
31	2B6	20.0	.	0.70	0.69	0.01	0.69	0.01
32	SV-17	9.0	0.640	0.62	0.67	-0.06	0.67	-0.05
33	2B15-1	0.0	.	0.68	0.67	0.01	0.66	0.01
34	S1A43-1	-15.0	.	0.64	0.66	-0.02	0.65	-0.02
35	2B15-2	-16.0	.	0.68	0.66	0.02	0.65	0.02
36	S1A33-1	-20.0	.	0.63	0.65	-0.03	0.64	-0.02
37	2B4-1	-20.0	.	0.64	0.65	-0.01	0.64	-0.01
38	2B4-2	-22.0	.	0.65	0.65	0.00	0.64	0.01
39	7002	-22.0	0.600	0.63	0.65	-0.02	0.64	-0.01
40	S1A44-1	-24.0	.	0.63	0.64	-0.01	0.63	-0.01
41	S1A43-2	-28.0	.	0.61	0.63	-0.02	0.62	-0.02
42	S1A33-2	-30.0	.	0.61	0.63	-0.02	0.62	-0.01
43	2A4	-30.0	.	0.64	0.63	0.01	0.62	0.02
44	S1A43-3	-31.0	.	0.62	0.62	-0.01	0.61	0.00
45	S1A44-2	-34.0	.	0.61	0.61	-0.00	0.60	0.00
46	S1A43-4	-38.0	.	0.60	0.60	0.01	0.59	0.02
47	S1A33-3	-39.0	.	0.57	0.59	-0.02	0.59	-0.01
48	SV-17T	-41.0	0.540	0.56	0.59	-0.03	0.58	-0.02
49	S1A33-4	-44.0	.	0.57	0.57	-0.00	0.57	0.01
50	SAN-SP-C	-44.5	0.540	0.56	0.57	-0.01	0.56	-0.00
51	1B1	-45.0	.	0.58	0.57	0.01	0.56	0.01
52	5A1	-50.0	.	0.56	0.54	0.02	0.54	0.02

standard deviations (*esd*) for the respective coefficients. Each indicates, as for the sigmoidal model, that if V_x equals 0° , then $\Sigma t_1 = 0.665$ (*esd* = 0.02). These equations predict that $2V_x$ will equal 57.6° for a completely disordered high sanidine ($\Sigma t_1 = 0.5$) and 86.7° for a completely ordered low microcline ($\Sigma t_1 = 1.0$). These compare to literature values of 54° and 82° . It should be noted that the largest $2V_x$ value reported for a sanidine, 63° , is for a

specimen synthesized by Tuttle (1952). Optically positive "isomicroclines" ($2V_x > 90^\circ$) were discussed in Footnote 2.

Linear model: Σt_1 versus $\tan^2 V_x$

Preiss (1981) and Ott (1982) found linear relationships for Σt_1 or t_1 and t_2 versus $\tan^2 V_x$ for suites of monoclinic K-rich feldspars between $2V_x \sim 50^\circ$ [OAP = (010)] and

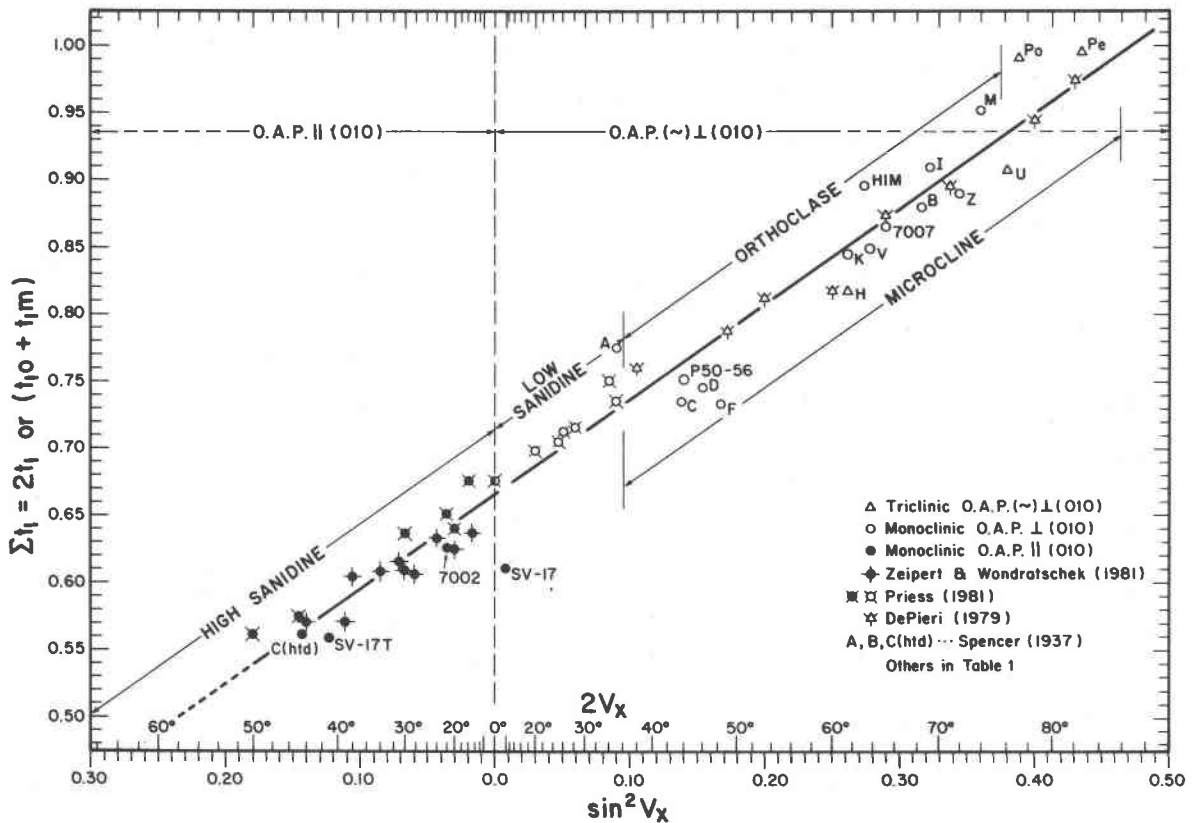


Fig. 4. $\sin^2 V_x$ and $2V_x$ versus Σt_i ; the Σt_i values were determined by the $[110], [1\bar{1}0]$ method of Kroll (1980, as discussed by Kroll and Ribbe, 1983). The line represents a least-squares regression fit to the data for 52 specimens in Table 1. See Equations 12a and b, and cf. Su *et al.* (1983b) for an earlier version.

$2V_x \sim 63^\circ$ [OAP \perp (010)]. We tested $\tan^2 V_x$ with our suite of 52 monoclinic and triclinic specimens and obtained an equation which may be split into two segments. For OAP = (010),

$$\Sigma t_i = 0.664(4) - 0.473(14) \tan^2 V_x, \quad (13a)$$

and for OAP \perp or nearly \perp to (010),

$$\Sigma t_i = 0.664(4) + 0.473(14) \tan^2 V_x, \quad (13b)$$

with $r^2 = 0.958$ and $esd = 0.03$ (just slightly higher than the esd of 0.02 for equation 12).

The rationale for near-linearity in the relationship between Σt_i and $\tan^2 V_x$ is similar to that for Σt_i and $\sin^2 V_x$, because equations similar to 8 through 11 can be derived for the $\tan^2 V_x$ function. The greater range of values of $\tan^2 V_x$ (from 0.0 to 1.0) accounts for the smaller r^2 and larger esd for equation 13 over equation 12.

Discussion and summary

Earlier work and partial birefringences

Finney and Bailey (1964, Fig. 2, p. 426) plotted the distant order function.

$$S = \sum_{i=1}^{i=4} \left[\frac{|0.25 - t_i|}{1.50} \right]$$

against $2V_x$ for all five structures of K-rich feldspars available at that time. Ribbe and Gibbs (1969, p. 86) recognized flaws in this and other distant order parameters and suggested that they be abandoned in favor of some more direct measure of the Al/(Al + Si) content of the tetrahedral sites (for example, those used by Weitz (1972) and DePieri (1979)). But Finney and Bailey's result was nonetheless an important contribution.

As may be demonstrated mathematically, S will be linearly related *only* to t_{10} when t_{1m} is < 0.25 , whereas, if $t_{1m} > 0.25$ or if the feldspar is monoclinic, S will be linearly related to Σt_i . Of course, Σt_i is the parameter we find to be rather precisely predictable from $2V_x$. Finney and Bailey (1964, Figs. 3 and 4) obtained a good non-linear correlation of $2V_x$ and "b"- α and a nearly perfect linear correlation of S and "b"- α , where the birefringence value "b"- α , as first proposed by Hewlett (1959), is equivalent to our $(n_b - n_a)$. Although they stated that their "diagrams should not be interpreted too vigorously . . . at this stage of our knowledge," Finney and Bailey's

ideas have proven to be correct. If we were to suggest a partial birefringence most sensitive to order-disorder in K-rich feldspars, it would be $(n_b - n_c)$, which passes through zero at $2V_x = 0$. Values for a Σt_1 versus $(n_b - n_c)$ plot may be derived from Figure 2.

Complete characterization of Al,Si distribution in triclinic K-feldspar

A measurement of $2V_x$ (or partial birefringence, $(n_b - n_c)$) permits easy determination of t_1 or $(t_{10} + t_{1m})$, and thus, using equation 3, of t_2 or $t_{20} = t_{2m}$. However, the individual Al contents of T_{10} and T_{1m} in triclinic potassic feldspars are *not* available from these measurements alone. Brown (1962, Fig. 2, p. 32) and Stewart (1974, Fig. 2, p. 158) suggested that the extinction angle α' or X' to the trace of (010) on (001) cleavage fragments may be linearly related to the difference $(t_{10} - t_{1m})$. A few data suggest a correlation between this extinction angle and the γ^* reciprocal lattice angle (Brown, 1962). In turn, γ^* is well known to be linearly correlated to $(t_{10} - t_{1m})$ (see Kroll and Ribbe, 1983, Fig. 5, p. 80). Marfunin (1966) hinted at the utility of angles between the individual optic axes and the normal to (010) in differentiating structural states of K-rich feldspars, but confirmation from lattice parameters or structure determination is lacking.

It is our intention to obtain complete optical *and* lattice parameter characterization of as many intermediate microclines as possible, so as to be able to fully characterize average Al,Si site distributions in triclinic potassic feldspars using rapid spindle or universal stage methods.

Unusual potassic feldspars

Bambauer and Laves (1960) studied a large (>1 cm) adularia "crystal" from Val Casatscha, Switzerland. This specimen exhibited coarse lamellar domains whose $2V_x$ angles and α^* and γ^* angles (recorded by X-ray precession methods) suggested a range of structural states from "(high) sanidine . . . (axial plane $\sim \parallel$ (010), $2V_x \approx 50^\circ$) . . . to microcline . . . (axial plane $\sim \perp$ (010), $2V_x \approx 50^\circ$). Between these extremes a continuous series of intermediate optical orientations was found" (p. 178). These unusual orientations, representing a range of intermediate microclines with triclinic symmetry, are *not* accommodated by our model. Carefully correlated structural, optical, and electron microscope studies of these and similar specimens are now under way to resolve the discrepancies.

Summary

Values of $2V_x$ measured for potassic feldspars in thin sections, plus the observations of whether $r < v$, which indicates the optic plane to be parallel to (010), or $r > v$, which indicates the optic plane to be perpendicular to (010) or nearly so, should suffice to determine t_1 and t_2 (for monoclinic) or $(t_{10} + t_{1m})$ and $t_{20} = t_{2m}$ (for triclinic crystals) from grain to grain (or point to point). Further

study is needed to confirm or establish more certainly the relationship between $(t_{10} - t_{1m})$ and extinction angles, especially $X' \wedge (010)$ on (001), which has the greatest potential. The K-rich feldspars of "unusual" optic orientation require special attention.

We urge that all investigators measure and report full optical orientation data for crystals on which structures are determined or that investigators in possession of such crystals (or for that matter, any known intermediate microclines) send them to FDB or PHR for further study.

Acknowledgments

The authors are grateful to numerous participants at the third NATO Advanced Study Institute on Feldspars and Feldspathoids for their stimulating discussions of this paper, especially Prof. H.-U. Bambauer. S. W. Bailey, Max Carman, and Elwood R. Brooks improved this paper with their reviews. This work was supported by National Science Foundation Grant EAR-8018492 to F. D. Bloss and D. R. Wones and EAR-8308308 to F. D. Bloss and P. H. Ribbe.

References

- Bailey, S. W. (1969) Refinement of an intermediate microcline structure. *American Mineralogist*, 54, 1540-1545.
- Bambauer, H. U. and Laves, F. (1960) Zum Adularproblem. I. Adular vom Val Casatscha: Mimetsicher Lamellenbau, Variation von Optik und Gitterkonstanten und ihre genetische Deutung. *Schweizerische Mineralogische und Petrografische Mitteilungen*, 40, 177-205.
- Blasi, A. (1972) \llcorner Iso-microclino \gg ed altre varanti strutturali del K-feldspato coesistenti in uno stesso cristallo nei graniti del Massiccio dell' Argentera (Alpi Marittime). *Rendiconti della Societa Italiana di Mineralogia e Petrologia*, 28, 375-411.
- Bloss, F. D. (1952) Relationship between density and composition in mol percent for some solid solution series. *American Mineralogist*, 37, 588-599.
- Brown, B. E. (1962) Aluminum distribution in an igneous maximum microcline and the sanidine microcline series. *Norsk Geologisk Tidsskrift*, 42, 25-36.
- Brown, B. E. and Bailey, S. W. (1964) The structure of maximum microcline. *Acta Crystallographica*, 17, 1391-1400.
- Cole, W. F., Sörum, H. and Kennard, O. (1949) The crystal structures of orthoclase and sanidinized orthoclase. *Acta Crystallographica*, 2, 280-287.
- Dal Negro, A., DePieri, R., Quareni, S. and Taylor, W. H. (1978) The crystal structures of nine K feldspars from the Adamello Massif (Northern Italy). *Acta Crystallographica*, B34, 2699-2707.
- DePieri, R. (1979) Cell dimensions, optic axial angle and structural state in triclinic K-feldspar of the Adamello Massif, Northern Italy. *Memorie di Scienze Geologiche*, Padova, 32.
- Finney, J. J. and Bailey, S. W. (1964) Crystal structure of an authigenic maximum microcline. *Zeitschrift für Kristallographie*, 119, 413-436.
- Gunter, M. and Bloss, F. D. (1982) Andalusite-kanonaite series: lattice and optical parameters. *American Mineralogist*, 67, 1218-1228.
- Hewlett, C. G. (1959) Optical properties of potassic feldspars. *Geological Society of America Bulletin*, 70, 511-538.
- Kroll, H. (1980) Struktur und Metrik der Feldspäte. *Habilitations-schrift*, Westfälische Wilhelms-Universität, Münster.

- Kroll, H. and Ribbe, P. H. (1983) Lattice parameters, composition and Al,Si order in alkali feldspars. In P. H. Ribbe, Ed., *Feldspar Mineralogy, Second Edition, Reviews in Mineralogy*, 2, 57-99. Mineralogical Society of America, Washington, D. C.
- Marfunin, A. S. (1966) The feldspars: phase relations, optical properties, and geological distribution. (Translated from the Russian edition, 1962). Israel Program for Scientific Translations, Jerusalem.
- Ott, G. (1982) Röntgenographische Strukturverfeinerungen an getemperten Eifelsanidinen zur Feststellung ihres Ordnungszustandes. Diplomarbeit, Institut für Kristallographie der Universität Karlsruhe.
- Phillips, M. W. and Ribbe, P. H. (1973) The structures of monoclinic potassium-rich feldspars. *American Mineralogist*, 58, 263-270.
- Priess, U. (1981) Untersuchungen zur Tief-Hoch-Umwandlung von Fe-haltigen Orthoklas-Kristallen aus Madagascar. *Neues Jahrbuch für Mineralogie, Abhandlungen*, 141, 17-29.
- Prince, E., Donnay, G. and Martin, R. F. (1973) Neutron diffraction refinement of an ordered orthoclase structure. *American Mineralogist*, 58, 500-507.
- Ribbe, P. H. and Gibbs, G. V. (1969) Statistical analysis and discussion of mean Al/Si-O bond distances and the aluminum content of tetrahedra in feldspars. *American Mineralogist*, 54, 85-94.
- Smith, J. V. (1974) *Feldspar Minerals. I. Crystal Structure and Physical Properties*. Springer-Verlag, Heidelberg.
- Spencer, E. (1937) The potash-soda feldspars. I. Thermal stability. *Mineralogical Magazine*, 24, 453-494.
- Stewart, D. B. (1974) Optic axial angle and extinction angles of alkali feldspars related by cell parameters to Al/Si order and composition. In W. S. MacKenzie and J. Zussman, Eds., *The Feldspars*, p. 145-161. Manchester University Press, Manchester.
- Stewart, D. B. and Ribbe, P. H. (1969) Structural explanation for variations in cell parameters of alkali feldspar with Al/Si ordering. *American Journal of Science*, 267-A, 144-462.
- Stewart, D. B. and Ribbe, P. H. (1983) Optical properties of feldspars. In P. H. Ribbe, Ed., *Feldspar Mineralogy, Second Edition, Reviews in Mineralogy*, 2, 121-139. Mineralogical Society of America, Washington, D. C.
- Stewart, D. B. and Wright, T. L. (1974) Al/Si order and symmetry of natural alkali feldspars, and the relationship of strained cell parameters to bulk composition. *Bulletin de la Société Française de Minéralogie et de Cristallographie*, 97, 356-377.
- Su, S. C., Bloss, F. D., Ribbe, P. H. and Stewart, D. B. (1983a) Rapid and precise optical determination of Al,Si ordering in potassic feldspars. Abstr. 3rd NATO Advanced Study Institute on Feldspars and Feldspathoids and Their Parageneses, Rennes, France.
- Su, S. C., Bloss, F. D., Ribbe, P. H. and Stewart, D. B. (1983b) Optic axial angle, a precise measure of Al,Si content of the T₁ tetrahedral sites in K-rich alkali feldspar. *Geological Society of America, Abstract with Programs*, 15, 000.
- Tuttle, O. F. (1952) Optical studies on alkali feldspars. *American Journal of Science, Bowen volume*, 553-567.
- Weitz, G. (1972) Die Struktur des Sanidins bei verschiedenen Ordnungsgraden. *Zeitschrift für Kristallographie*, 136, 418-426.
- Wright, T. L. and Stewart, D. B. (1968) X-ray and optical study of alkali feldspar: I. Determination of composition and structural state from refined unit-cell parameters and 2V. *American Mineralogist*, 53, 38-87.
- Zeipert, C. and Wondratschek, H. (1981) Ein ungewöhnliches Temperverhalten bei Sanidin von Volkesfeld/Eifel. *Neues Jahrbuch für Mineralogie Monatshefte*, 407-415.

*Manuscript received, August 30, 1983;
accepted for publication, December 13, 1983.*